# SmartFSCV: An Artificial Intelligence Enabled Miniaturised FSCV Device Targeting Serotonin

Dean M. Corva, *Member, IEEE*, Egan H. Doeven, Brenna Parke, Scott D. Adams, *Member, IEEE*, Susannah J. Tye, Parastoo Hashemi, Michael Berk, and Abbas Z. Kouzani, *Member, IEEE*

***Abstract*—*Goal:*** **Dynamically monitoring serotonin in real-time within target brain regions would significantly improve the diagnostic and therapeutic approaches to a variety of neurological and psychiatric disorders. Current systems for measuring serotonin lack immediacy and portability and are bulky and expensive. *Methods:* We present a new miniaturised device, named SmartFSCV, designed to monitor dynamic changes of serotonin using fast-scan cyclic voltammetry (FSCV). This device outputs a precision voltage potential between −3 to +3 V, and measures current between −1.5 to +1.5 $\mu$A with nano-ampere accuracy. The device can output modifiable arbitrary waveforms for various measurements and uses an N-shaped waveform at a scan-rate of 1000 V/s for sensing serotonin. *Results:* Four experiments were conducted to validate SmartFSCV: static bench test, dynamic serotonin test and two artificial intelligence (AI) algorithm tests. *Conclusions:* These tests confirmed the ability of SmartFSCV to accurately sense and make informed decisions about the presence of serotonin using AI.**

***Index Terms*—Artificial intelligence, electrochemistry, device, fast-scan cyclic voltammetry, serotonin.**

***Impact Statement*—Ultimately, SmartFSCV is the first step to a portable serotonin sensing platform with the ability to make on-board decisions. SmartFSCV shows potential for understanding and treating neurological and psychiatric disorders.**

Manuscript received 10 November 2023; revised 2 January 2024 and 15 January 2024; accepted 16 January 2024. Date of publication 19 January 2024; date of current version 23 February 2024. The work of Michael Berk was supported by the NHMRC Senior Principal Research Fellowship and Leadership 3 Investigator under Grants 1156072 and 2017131. The review of this article was arranged by Editor Danilo Demarchi. *(Corresponding author: Abbas Z. Kouzani.)*

Dean M. Corva, Scott D. Adams, and Abbas Z. Kouzani are with the School of Engineering, Deakin University, Geelong, VIC 3216, Australia (e-mail: d.corva@deakin.edu.au; scott.adams@deakin.edu.au; kouzani@deakin.edu.au).

Egan H. Doeven is with the School of Life and Environmental Sciences, Deakin University, Geelong, VIC 3216, Australia (e-mail: egan.doeven@deakin.edu.au).

Brenna Parke and Parastoo Hashemi are with the Department of Bioengineering, Imperial College London, SW7 2AZ London, U.K. (e-mail: b.parke20@imperial.ac.uk; phashemi@imperial.ac.uk).

Susannah J. Tye is with Queensland Brain Institute, The University of Queensland, St. Lucia, QLD 4072, Australia (e-mail: s.tye@uq.edu.au).

Michael Berk is with the School of Medicine, IMPACT, Deakin University, Geelong, VIC 3216, Australia (e-mail: michael.berk@deakin.edu.au).

Digital Object Identifier 10.1109/OJEMB.2024.3356177

## I. Introduction

SEROTONIN or 5-hydroxytryptamine (5-HT) is a monoamine neurotransmitter that is thought to regulate many different behavioural and cognitive processes, in particular memory and mood [1]. Serotonin activity is mediated by seven 5-HT receptors (5-HTRs), located in both the central nervous system (CNS) and peripheral nervous system (PNS), interacting with other neurotransmitters and ligands, such as dopamine, epinephrine, $\gamma$-aminobutyric acid (GABA), cortisol, prolactin, acetylcholine (ACh), oxytocin, substance P, and vasopressin [1], [2]. Dysregulation of the serotonin system is thought to be important in the pathology of psychiatric disorders such as major depressive disorder (MDD) [3], [4], [5], [6]. Selective serotonin reuptake inhibitors (SSRIs) block serotonin reuptake, ostensibly increasing the extracellular levels of serotonin within the CNS and are used extensively clinically for MDD, obsessive–compulsive disorder (OCD) [7], [8], anxiety disorders [9], post-traumatic stress disorder (PTSD) [10], and borderline personality disorder (BPD) [11]. Furthermore, SSRIs have been used to treat alcohol use disorder (AUD) [12], nicotine and other substance use disorders [9], [13]. Because of the variable clinical efficacy of SSRIs, the long time frame (weeks) for clinical benefits and stagnation in developing improved SSRIs, [14], the community has turned to other treatments such as ketamine [15], psychedelics [16] and deep brain stimulation (DBS) [17], [18], [19]. However, none of these alternative therapies currently show clinical outcomes that are an improvement on SSRIs.

A major barrier for improving depression therapies is the lack of understanding of the neurochemical pathology underlying the disease. An excellent step towards improving our understanding is to study the precise mechanisms of antidepressants and other modalities on the serotonergic system. This research requires the ability to accurately measure serotonin levels in vivo and in vitro.

Measuring analyte “fingerprints” such as serotonin, from the complex brain environment has proven difficult. Currently, serotonin can be sensed using spectrophotofluorometry [20], gas and liquid chromatography [21], mass spectrometry [22], capillary electrophoresis [23] and positron emission tomography [24]. However, these methods are often complex and difficult to miniaturise, limiting experiments to bench-top applications.

Fast-scan cyclic voltammetry (FSCV) is an electrochemical technique used for measuring serotonin [25], and is a mature method to directly sense extracellular levels of neurotransmitters on a sub-second timescale in discrete brain regions [26]. FSCV increases analyte selectivity, in-turn allowing researchers to monitor neurochemical dynamics and concentrations in real-time [27]. FSCV is a sub-category of cyclic voltammetry (CV), that uses two electrodes: working (WE) and reference electrodes (RE). FSCV typically operates by sweeping a voltage potential between the two electrodes, often including a pre-concentration step, effectively oxidizing, and reducing analytes at the surface of the WE. Redox active analytes then induce a current at a specific applied potential point, which can be identified and quantified [28].

Currently, the majority of FSCV-based research is performed using standalone commercially available benchtop equipment [29]. Recent advancements in electronics have enabled FSCV to be miniaturised [30], allowing portability for chemically sensitive devices to measure neurotransmitter concentrations in vivo [31]. For example, the wireless instantaneous neurotransmitter concentration system (WINCS) [32] developed by the Mayo Clinic (USA) is a miniaturised FSCV device that wirelessly sends data to a nearby computer using Bluetooth. Similarly, Pinnacle Technology's wireless FSCV system for rats [33] is a miniaturised FSCV device that communicates using Bluetooth. The downside to these systems is that they require transferring data to a nearby computer and can be costly. Adams et al. [34] developed a lower cost alternative called TinyFSCV, however, this system requires tethering to a computer to transfer data, and has a maximum scan rate of 400 V/s, too slow for measuring serotonin. Processing data on-board of the device would mitigate the need to transfer data to an external computer, simplifying device complexity and allowing the device to be truly miniaturised. Bozorgzadeh et al. [35] developed the neurochemostat, a miniaturised FSCV device with on-board data processing capabilities, however, this device is also focused on sensing for dopamine at a scan rate of 400 V/s.

In this work, we present a new miniaturised FSCV device for the detection of serotonin using AI. Currently, no miniaturised FSCV device has been developed with artificial intelligence (AI) capabilities, opening the door to new measurement possibilities that could rapidly inform human circuit therapeutic approaches. This device is constructed using discrete components, lowering the cost significantly than other devices that have been reported in the literature using ASIC construction. The device is battery powered and has the capability to process data on-board, requiring no wired connection to a computer.

## II. Materials and Methods

### A. Hardware

SmartFSCV was designed to detect rapid changes of serotonin. It uses discrete components on a custom 6-layer printed circuit board (PCB). The device is designed to output a voltage potential of between $-3$ to $+3$ V using a 2-electrode configuration, and measures current between $-1.5$ to $+1.5$ $\mu$A with nanoampere scale resolution. SmartFSCV requires power from two batteries in a split rail configuration. This enables SmartFSCV to have both positive and negative rails in a linear configuration, which also maintains simplicity, as typical split rail supplies require some form of a switching circuit if operated from a single voltage supply. SmartFSCV can operate in two different modes: standalone and tethered. Standalone uses on-board AI and requires no external connections, and tethered is for connection to an external computer to transfer data if required. There are four key components to SmartFSCV's hardware: waveform generation, current measurement, processing, and power supply. A simplified circuit diagram for SmartFSCV is shown in Fig. 1, which also excludes the power supply. The power supply is discussed in Section B, Power Supply.

***1) Processor:*** SmartFSCV uses an STM32H747XI by STMicroelectronics, an advanced 32-bit dual-core microcontroller. The STM32H747 operates both an ARM Cortex-M7 core at 480 MHz and an ARM Cortex-M4 core at 240 MHz. These processing speeds are necessary for operating the device at high scan rates. In addition, SmartFSCV uses an MX25L12833FZ2I as flash memory. Furthermore, SmartFSCV has a USB3320C and accompanying USB-C connector, to interface the device to a nearby computer using the USB serial communication. An on-board configurable red-green-blue (RGB) LED is used for feedback when the device is in standalone operation.

***2) Power Supply:*** SmartFSCV operates using a bipolar power supply, as FSCV requires bipolar output potentials across the electrodes. In addition, SmartFSCV is required to measure bipolar currents. For this reason, a two-battery configuration was decided to be the most efficient method of supplying clean power. SmartFSCV was designed to accept two 9 V, alkaline batteries or two A23, 12 V, alkaline batteries. This decision was based around the accessibility and low cost of these batteries, approximately $4.94 AUD for a two pack of A23 batteries. This provides SmartFSCV with an input supply of either $\pm$12 V or $\pm$9 V. SmartFSCV then filters this input supply using 9 positive and negative linear regulators. The first $\pm$5 V rail supplies power to the waveform generation circuit, using an ADP7118AUJZ-5.0 for the $+$5 V supply, and an ADP7182AUJZ-5.0 for the –5 V supply. The second $\pm$2.5 V rail supplies power to the current measurement circuit, using an ADP7142AUJZ-2.5 for the $+$2.5 V supply, and an ADP7182ACPZN-2.5 for the –2.5 V supply. Other linear regulators used include an LP5907-3.1, ADP7142AUJZ-1.8 and AP7331-1.2, which supply $+$3.1 V, $+$1.8 V and $+$1.2 V to the processor. In addition, an ADP3330ARTZ-3.3 supplies $+$3.3 V to the digital part of the waveform generation and current measurement circuit. Furthermore, an AP2138N-3.0 supplies $+$3 V to the relay control circuit.

***3) Waveform Generation:*** FSCV requires the ability to accurately set and sweep a precise voltage potential between the WE and RE. Key FSCV parameters include minimum voltage, maximum voltage, holding voltage, and scan rate, which defines how fast the voltage is being altered. These parameters are altered depending on the target analyte. From the current literature [36], sensing serotonin optimally requires a scan-rate of 1000 V/s, a minimum voltage of $-0.1$ V, a maximum voltage of $+1$ V, and a holding voltage of $+0.2$ V. This scan rate is much

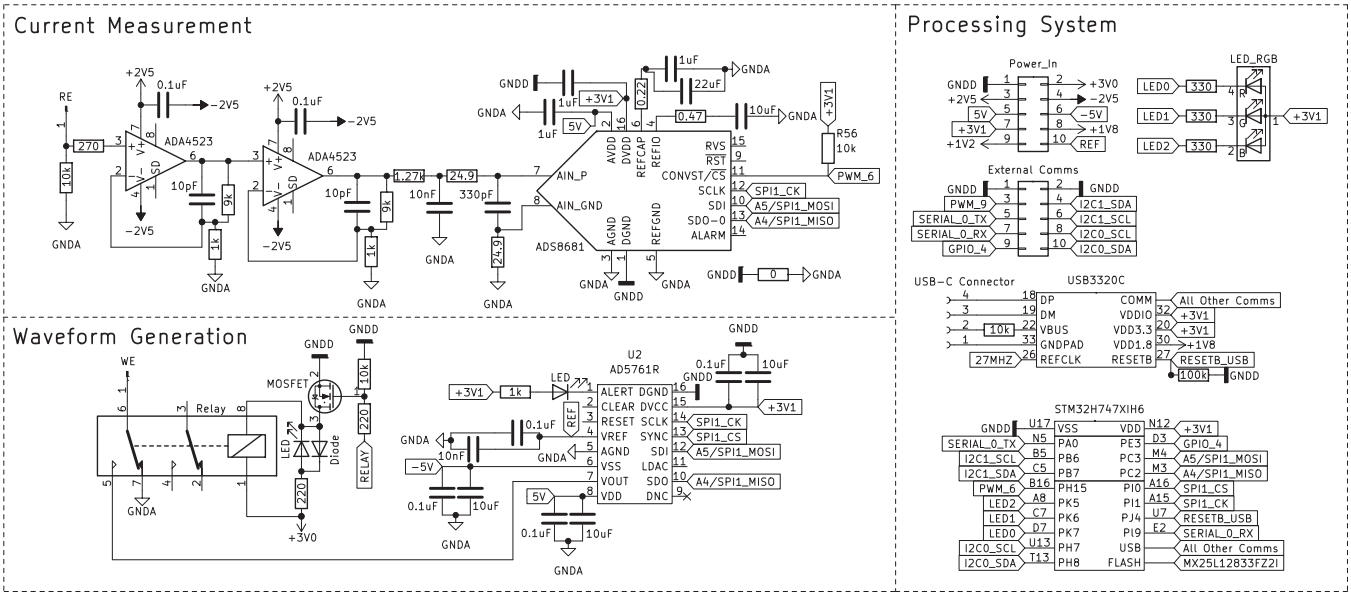


**Fig. 1.** Simplified circuit diagram of SmartFSCV (revision 2.0).

higher than scan rates used for other analytes such as dopamine, which are typically scanned at 400 V/s. For this reason, developing an FSCV device capable of both outputting and measuring at 1000 V/s has increased complexities. In addition, sensing serotonin optimally uses an N-shape "Jackson" waveform [36], which is more complex than a two-sloped, triangle shaped, FSCV waveform.

SmartFSCV uses an AD5761R for the waveform generation, a 16-bit, external, digital-to-analogue converter (DAC). SmartFSCV communicates to the AD5761R using serial-peripheral interface (SPI). This DAC has the capability to be set for bipolar operation through software configuration. SmartFSCV operates the AD5761R using the selected $\pm 3$ V range. This provides enough headroom to meet the required $-0.1$ V to $+1$ V for serotonin. The output of the DAC feeds directly into a miniature relay, for isolating the output. This is crucial to guarantee a proper isolation of the electrode potential from the electrochemical cell when not in operation. When powered off, the electrode is referenced to virtual ground. Operating the AD5761R from an external reference increases its accuracy, for example, the gain error using the internal reference is $\pm 0.15$ % FSR, whereas using an external precision reference reduces this to $\pm 0.1$ % FSR. For this reason, an REF6025 (Texas Instruments, USA), a $+2.5$ V voltage reference is used.

***4) Current Measurement:*** To precisely quantify the target analyte, an FSCV system requires a highly accurate current measurement within the nano-ampere range. The measured current is a combination of faradaic and capacitive current. Faradaic current is the result of reduction and oxidation of target analytes at the electrodes, while capacitive current is when the electrode tip is undergoing capacitive double layer charging. Both currents are affected by scan-rates produced by the FSCV system.

The first section of the current measurement circuit on SmartFSCV is a precision 10 kΩ current shunt resistor. This precision resistor is in series with the reference electrode. A 0.01% tolerance precision resistor was selected to simplify the current to voltage conversion process.

The second section is a 2-stage, 100X gain, non-inverting amplification circuit. This section converts the cell current to a voltage drop using the precision current shunt resistor and amplifies it by 100X. This section uses two ADA4523-1 by Analog Devices. This amplifier has low input bias current (typically 200 pA), low offset voltage (typically $\pm 0.5$ $\mu$V) and a common-mode rejection ratio (CMRR) of 146 dB, making it ideal for a low-noise amplification circuit.

The third stage is a low pass filter, using a 1 kΩ resistor and 10 nF capacitor in a 1$^{st}$ order resistive-capacitive ($RC$) configuration. The cut-off frequency ($F_C$) is determined by using (1), which for SmartFSCV is approximately 16 kHz.

$$F_C = \frac{1}{2\pi RC} \tag{1}$$

The final stage of the current measurement circuit is the analogue-to-digital convertor (ADC), which converts the measured analogue voltage into a digital signal, readable for the processing system. SmartFSCV uses an ADS8681 by Texas Instruments (USA), a 1MSPS, 16-bit, successive approximation (SAR) ADC. This ADC can operate using a single $+5$ V supply and supports true bipolar input ranges. SmartFSCV operates the input range of the ADS8681 at $\pm 2.56$ V. SmartFSCV communicates to the ADS8681 using SPI.

***5) Fabrication:*** Fabrication of the device was performed on-site at Deakin University. The COVID-19 pandemic created a shortage of electronic components, therefore, developing the device limited by only selecting parts that were available during development. This is exemplified by some parts being de-soldered from development boards and re-soldered onto SmartFSCV. For this reason, SmartFSCV could have its size and cost further reduced, as ideal component packages and lower cost alternatives could be used.

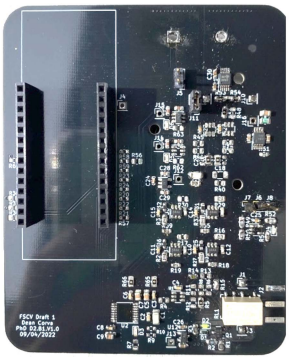

(a). Circuit Board of Revision 1.0 (April 2022).

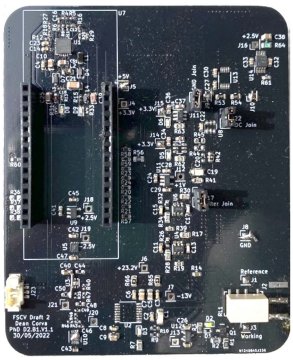

(b). Circuit Board of Revision 1.1 (May 2022).

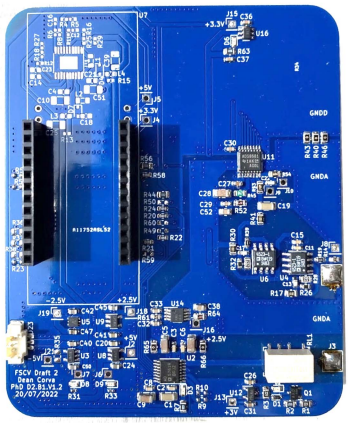

(c). Circuit Board of Revision 1.2 (July 2022).

**Fig. 2.** Revision 1 of SmartFSCV (76 mm × 93 mm).

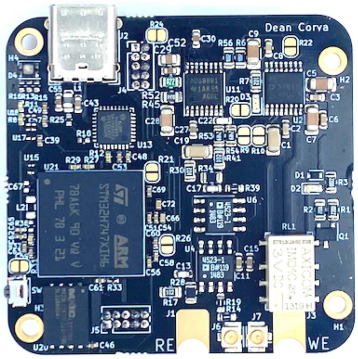

(a). Main FSCV PCB

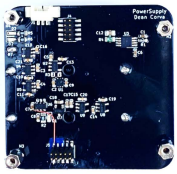

(b). Power Supply PCB Front

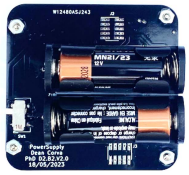

(c). Power Supply PCB Rear

(d). Main FSCV PCB

**Fig. 3.** Revision 2.0 (December 2022).

***6) Revisions:*** SmartFSCV underwent multiple revisions prior to the final version. The first 3 revisions used a Portenta H7 development board and were constructed using a 2-layer PCB (76 mm × 93 mm). The final revision uses all discrete components on a 6-layer PCB (46 mm × 47 mm). Revision 1.0 (April 2022), shown in Fig. 2(a), operated using a single battery as the power supply, using a single op-amp to split a +9 V battery into ±4.5 V. In addition, it used an ADS8860 for the ADC, which required an additional 4$^{th}$ section after the low-pass filter, of a unity gain buffer circuit with a +1 V DC bias offset. This was implemented to shift the bipolar waveform into the positive domain, as the ADS8860 only accepts values above 0 V. To prevent the DC bias from injecting into the non-inverting amplifier section, an AC coupling capacitor was placed prior to the input.

Revision 1.1 (May 2022), shown in Fig. 2(b), changed the power supply from a single battery and op-amp to an ADP5070ACPZ, a DC-to-DC switching regulator that accepts a +5 V input and outputs a maximum ±39 V. This increased the headroom and stability of the power supply and enabled the device to be completely powered from a USB source. In addition, an external power supply port was added, enabling the device to be powered from two 9 V, alkaline batteries.

Revision 1.2 (July 2022), shown in Fig. 2(c), changed the ADC from the ADS8860 to the ADS8681, removing complexities associated with the unity gain buffer circuit. In addition, this revision changed the op-amps to the ADA4523-1 and had significant improvements in the PCB design for the analogue front-end, compensating for capacitive coupling in the tracks. This increased the signal-to-noise ratio of the device.

Revision 2.0 (December 2022), shown in Fig. 3(a) and (d), is a miniaturised version of revision 1.2 and uses only discrete components. In addition, it removed any unnecessary testing components from the design phase. It has a 6-layer construction, gold plating, castellated edges, separate analogue and digital ground planes, separate output waveform and current measurement sections, and external communication and power ports. Revision 2.0 uses a separate PCB for the power supply, shown in Fig. 3(b) and (c), which is interfaced using connectors between the two PCBs. In addition, it adds ultra-small FL (U.FL) connectors (Hirose Electric Group) for interfacing electrodes using a shielded cable.

## B. Software

SmartFSCV operates two key pieces of software: the firmware for operating the device, and the AI software for reading and analysing the data. The device firmware controls the DAC for the waveform generation and the ADC for the current measurement. In addition, it handles the optional communication to a nearby computer using a wired connection, if the user elects to see the voltametric data. The AI algorithm handles all the analysis aspects of the device, deciding if SmartFSCV is sensing serotonin. Fig. 4 shows the program flow including the

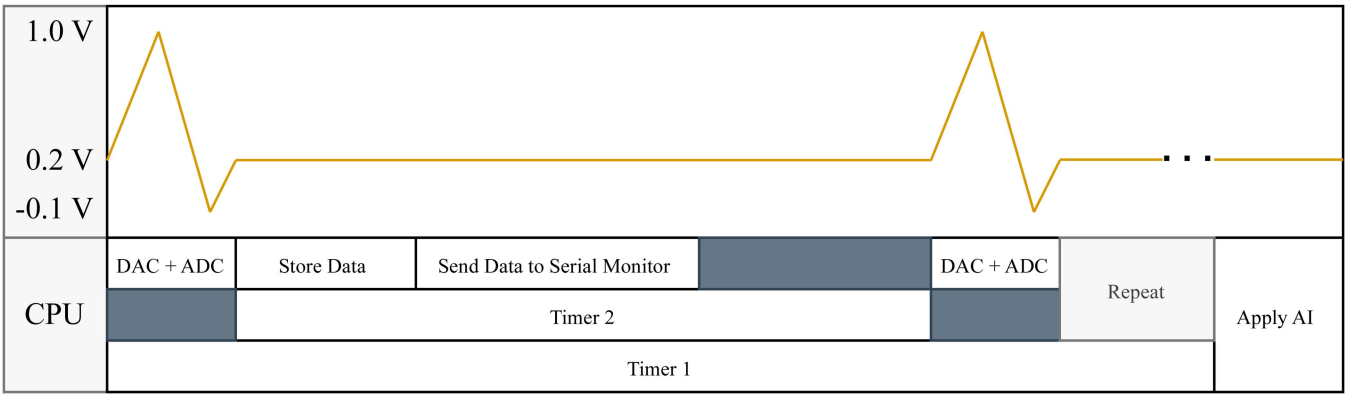


**Fig. 4.** Software of SmartFSCV.

waveform output. As the DAC increments, the ADC samples, and stores values. Once complete, the holding voltage phase of the waveform allows the software to store the previous ADC values and send data to serial monitor if serial connected.

***1) Firmware:*** SmartFSCV's firmware is programmed in C and follows several key steps. The first step is to initialise the system, following this sequential order: set timers, initialise the serial port, enable the SPI communication, and initialise functions. Once complete, an on-board LED is turned on, relay circuit closed, and timer 1 begins (main code duration timer). The second step enters the main code following this sequential order: increment DAC value, sample ADC value, repeat until waveform complete, begin timer 2, store data in memory, send data to serial monitor, wait for timer 2 to complete, repeat all steps. Fig. 5 displays the pseudocode for SmartFSCV.

***2) Artificial Intelligence:*** Machine learning (ML) is a form of AI that turns raw data into meaningful information at an application level. ML is excellent for solving problems that involve pattern recognition that are difficult for the human observer to identify. In this case, removing the need for post data processing to identify the serotonin sample within the buffer solution.

To create an ML program, a set of training data is first required. ML then uses an algorithm to learn rules from the training data. In addition, a pre-processing block can be used for filtering the signal prior to the algorithm. Many pre-processing blocks were tested and compared against, such as flattening the axis, spectral analysis, and spectrogram, however, using no pre-processing block (raw data) returned the best results. Algorithms were also compared, such as regression and anomaly detection (K-means), with a classification algorithm (Keras [37]) returning the best results. Settings for the neural network include a 5-layer architecture of input layer (354 features), dense layer (30 neurons), dense layer (30 neurons), dense layer (30 neurons) and an output layer. Both preliminary and secondary algorithms were developed and trained using Edge Impulse [38], which allows users to export as C code. The datasets used for training the algorithms are described in Section III, Results and Discussion. This code is then adapted into SmartFSCV's main firmware and is called as a function in the main loop. The training data is not updated after the model is developed and deployed into the device.

```
START
{
        initialise_Timers();
        initialise_Serial();
        initialise_SPI();
        initialise_Functions();

        LED_On();
        Relay_On();                 // Close Output Relay
        Timer_1_Start();            // Main Timer

        main()
        {
                while (Waveform)    // Serotonin Waveform
                {
                        DAC_Increment();
                        ADC_Sample();
                }
                Timer_2_Start();
                Store_Memory();
                Send_Serial();
                while (Timer_2);    // Wait for Timer 2
                if (Waveform == n Samples)
                {
                        AI_Start();     // Do AI analysis
                }
        }
}
```

**Fig. 5.** SmartFSCV pseudocode.

## C. Electrochemistry Setup

All chemicals used for testing SmartFSCV were purchased from Sigma Aldrich, Australia. Water used was purified to > 18.6 MΩ/cm using a Merck Millipore (Merck, USA) water purifying system. A 10x Tris buffered saline (pH 7.4) stock buffer solution (consisting of Trizma HCl (200 mM), NaCl (1.41 M), KCl (32.5 mM), $CaCl_2$ (13.3 mM), $NaH_2PO_4{\cdot}2H_2O$ (10.0 mM), $MgCl_2$ (12.2 mM), and $Na_2SO_4$ (20.2 mM)) was made up in H2O and diluted by a factor of 10 before use. A 1 mM stock serotonin HCl solution was prepared freshly the day of experiments, which was diluted to various concentrations in 1X TRIS buffer as required before use. The serotonin solutions

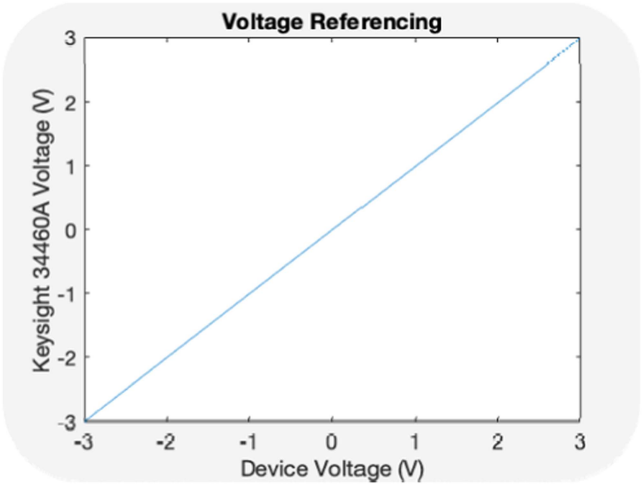


Fig. 6. Voltage referencing of SmartFSCV to a keysight 34460A.

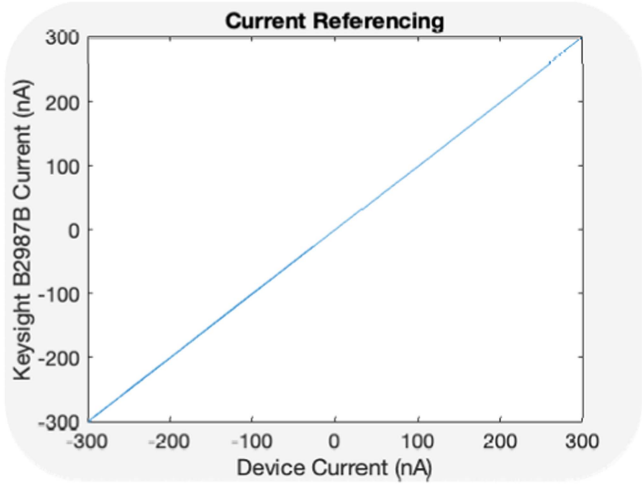


Fig. 7. Current referencing of SmartFSCV to a keysight B2987B.

were shielded from light. A 7 $\mu$m diameter carbon fiber microelectrode (CFM) and 600 $\mu$m diameter Ag|AgCl reference electrode was used for FSCV experiments. CFMs were fabricated at Imperial College London by aspirating a carbon fiber (7 $\mu$m diameter, T-650, Goodfellow) into a borosilicate glass capillary (1.0 mm outer diameter $\times$ 0.68 mm inner diameter $\times$ 100 mm long, science-products, Germany). A carbon-glass seal was forged under heat and gravity with a vertical pipette puller (PE-22, Narishige, Tokyo, Japan) and the protruding carbon fiber cut to 150 $\mu$m in length. An electrical connection was made by putting a pinned stainless-steel wire coated in silver paint through the opposite end of the capillary. The reference electrode was fabricated by electrochemically coating a silver wire with AgCl (5 min at 5 V in 0.1M HCl).

Experiments were conducted using a custom made flow cell [39] (Imperial College, London), a 6-port valve (Valco Instruments), PEEK tubing (VICI Valco Instruments Inc. TPK140) with 170.25 $\mu$L volume sample loop and syringe pump (Harvard Apparatus Standard PHD ULTRA CP Syringe Pump). Comparative FSCV experiments were performed using an Autolab 128N potentiostat with ADC10M and SCANGEN250 modules installed (Metrohm, NL). Experiments were conducted in a faraday cage (Gamry Instruments).

## III. Results and Discussion

To validate SmartFSCV, the following four experiments were conducted: (1) FSCV of static loads, (2) FSCV of dynamic serotonin, (3) Preliminary AI results of dynamic serotonin and (4) Secondary AI analysis results of dynamic serotonin.

### A. Experiment 1: Static Resistive Referencing

Prior to validating a voltammetry system via electrochemical measurements, bench-testing the system to ensure that it outputs a precise voltage and measures an accurate current is paramount to success. Fig. 6 is the result of sweeping the maximum output potential of SmartFSCV and measuring using a Keysight 34460A benchtop multimeter. Fig. 7 is the result of sweeping the maximum output potential of SmartFSCV across a precision 10 M$\Omega$ resistor and measuring using a Keysight B2987B benchtop picoammeter. During these tests the ambient temperature ranged between 21.7 °C to 22.2 °C. Fig. 8 shows the experimental setup.

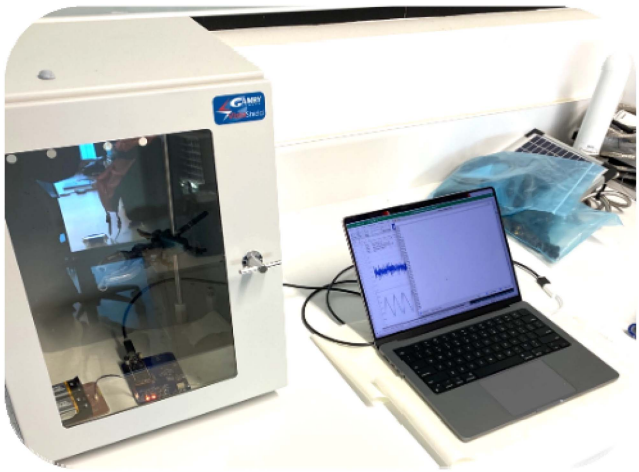

Fig. 8. Experiment 1 setup: Static resistive referencing.

This referencing clearly demonstrates the precision and linearity of the SmartFSCV's voltage generation and current measurement. A maximum deviation of $\pm$1 nA and $\pm$1 mV was measured during the referencing.

Specifications of SmartFSCV were determined from this referencing. They are listed in Table I.

### B. Experiment 2: FSCV of Dynamic Serotonin

The second experiment evaluates SmartFSCV's ability in a neurochemical sensing application, by measuring dynamic changes in serotonin concentration. Equipment used in this experiment follows that listed in Section IV, Electrochemistry Setup. Prior to experimentation, buffer solutions were allowed to adjust to room temperature. First, both electrodes were mounted

**TABLE I**
SPECIFICATIONS OF SMARTFSCV

| | |
|---|---|
| Channels | 1 |
| Cell Potential Range | -3 to +3 V |
| Cell Current Range | -1 to +1 μA |
| Output Resolution | 16-bit |
| Input Resolution | 16-bit |
| Max Scan Rate | 1000 V/s |
| Battery Voltage | 9 – 12 V |

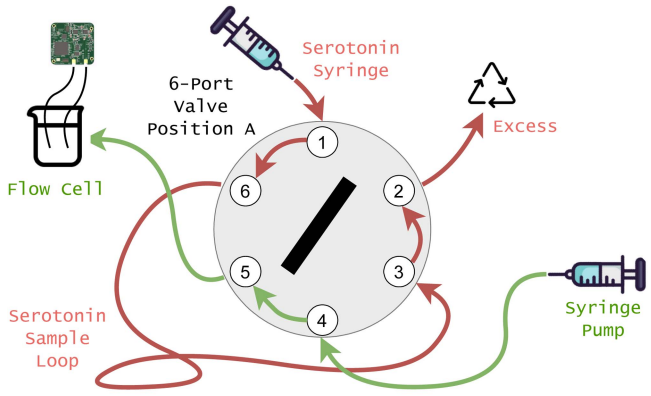


(a). Position A.

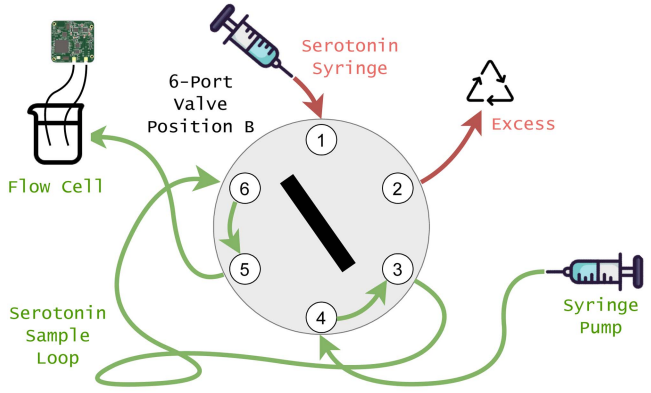


(b). Position B.

**Fig. 9.** Experiment 2 Setup.

to the flow cell, followed by connection of all the tubing to the syringes, valve and flow cell. The syringe pump was loaded with TRIS buffer and sample loop loaded with 170.25 $\mu$L of diluted serotonin solution.

Position A of the valve, shown in Fig. 9(a), excludes the serotonin loop, supplying only TRIS buffer to the flow cell. Position B, shown in Fig. 9(b), injects the loaded serotonin within the sample loop into the flow cell.

Prior to measurement using SmartFSCV, we adjusted the electrodes using the Autolab 128N while running TRIS buffer to ensure the measured current was less than the maximum current rating of SmartFSCV. This step added complexity as micrometre adjustments significantly increased the measured current. Once complete, SmartFSCV was then connected to the electrodes. Experimental setup is shown in Fig. 10.

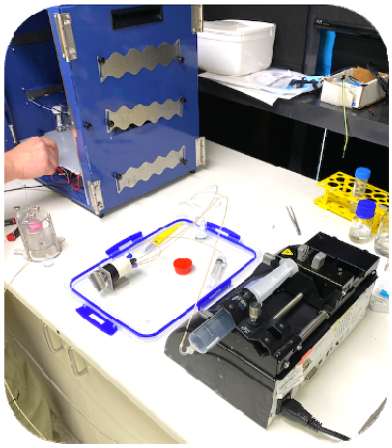

(a). Experiment 2 Setup: Faraday Cage, Syringe Pump, 6-Port Valve and Flow Cell.

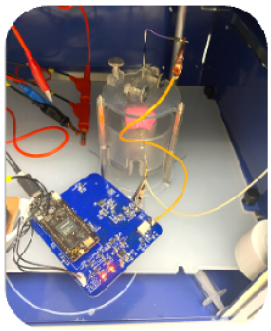

(b). Experiment 2 Setup: Flow Cell and SmartFSCV inside Faraday Cage.

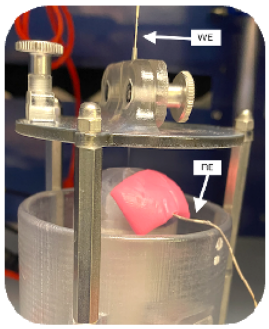


(c). Experiment 2 Setup: WE and RE Electrodes in Flow Cell.

**Fig. 10.** Experiment 2 setup.

The voltage waveform for the experiment was scanned from a holding voltage of +0.2 V to +1.0 V to −0.1 V and back to +0.2 V, at a scan rate of 1000 V/s. A preconditioning step was performed prior to experimental use, cycling the waveform at 60 Hz for 10 minutes in position A, then at 10 Hz for another 10 minutes, to equilibrate the electrode and minimize background current drift. The flow rate of the syringe pump was set to 1 mL/min. Once SmartFSCV collected enough buffer samples, switching the 6-port valve to position B injected the serotonin sample into the flowing stream. Two samples were taken from SmartFSCV's results, one buffer and one mid serotonin injection (100 nM) and were processed in MATLAB using a Gaussian filter to show the voltammogram pre- and post-serotonin injection, although not necessary for the AI processing, displayed in Fig. 11.

Although the processed results are not necessary for the AI algorithm, it aids in the visualisation of the faradaic current peak. The current responses to buffer and serotonin at the electrode are plotted against the voltage applied and are typical of those expected for serotonin CV's (oxidation at 0.7 V and reduction at 0 V), indicating serotonin redox at the electrode. Subtracting the serotonin CV from the buffer CV resulted in a measured oxidation peak of 15 nA across 1 electrode for a 100 nM injection of serotonin.

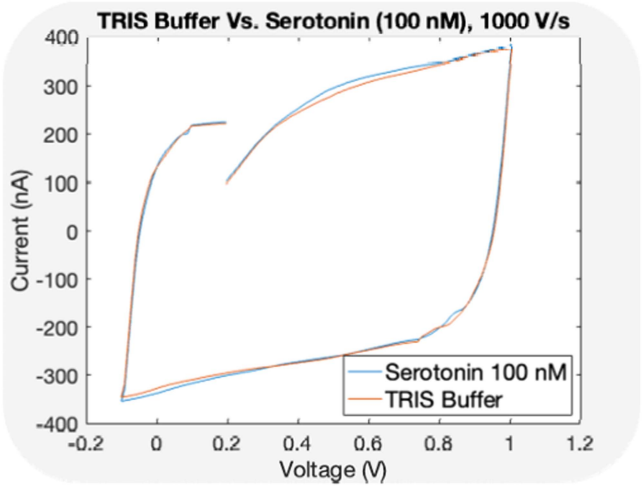


**Fig. 11.** SmartFSCV experiment 2 CV plot: TRIS buffer vs. serotonin (100 nM), 1000 V/s.

**TABLE II**
TRAINING DATA CONFUSION MATRIX FOR PRELIMINARY AI

| | Buffer | Serotonin |
|---|---|---|
| Buffer | 100% | 0% |
| Serotonin | 0% | 100% |
| F1 Score | 1.00 | 1.00 |

### C. Experiment 3: Preliminary AI Detection of Serotonin

The third experiment evaluates the effectiveness of the AI to detect a dynamic serotonin response. First, an AI algorithm is trained on a computer using gathered data. Then, the trained model is loaded into the device's firmware. The user can export the outputs of the model using tethering. In our case, we exported the testing data to plot the feature explorer. The user may elect to use standalone operation requiring no tethering by using the on-board RGB LED (e.g., green light for serotonin present, red light for not present).

A preliminary AI algorithm was developed using the unfiltered raw current measurements from Experiment 2. Output layers for this algorithm use 2 classes (serotonin present and no serotonin present) to identify and classify the 15 nA faradaic oxidation current. The dataset contained 11 serotonin samples and 10 buffer samples. Splitting the data 76% for training and 24% for testing was determined to be the best ratio. The unfiltered raw data is time series based with a measurement window of 1 ms per sample. Several training cycles and learning rates were tested to find the best AI performance results. This resulted in 200 training cycles and a learning rate of 0.0001. An example of single serotonin raw data sample is displayed in Fig. 12. Training results from the preliminary AI algorithm are displayed in Table II and Fig. 13 using 7 buffer samples and 8 serotonin samples. Testing results from the preliminary AI algorithm are displayed in Table III and Fig. 14 using 2 buffer samples and 2 serotonin samples.

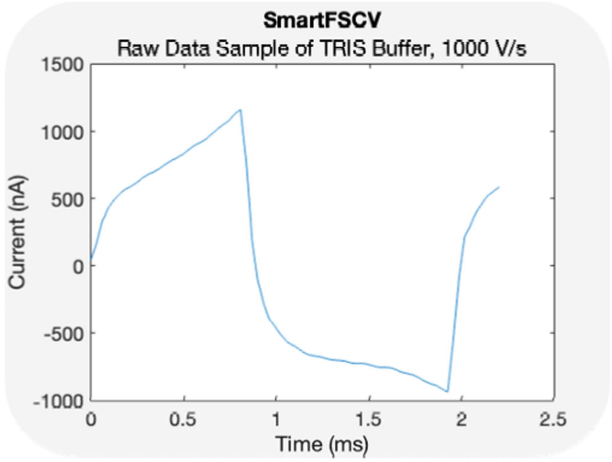


**Fig. 12.** Raw data sample of TRIS buffer current measurement.


**Fig. 13.** Experiment 3: Preliminary AI training feature explorer using 7 buffer samples and 8 serotonin samples.

**TABLE III**
TESTING DATA CONFUSION MATRIX FOR PRELIMINARY AI

| | Buffer | Serotonin |
|---|---|---|
| Buffer | 100% | 0% |
| Serotonin | 0% | 100% |
| F1 Score | 1.00 | 1.00 |

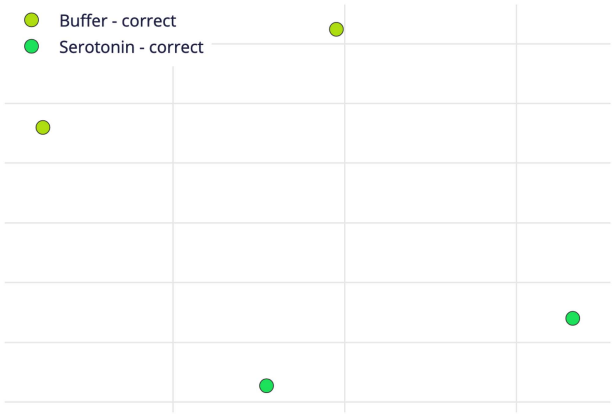


**Fig. 14.** Experiment 3: Preliminary AI testing feature explorer using 2 buffer samples and 2 serotonin samples.

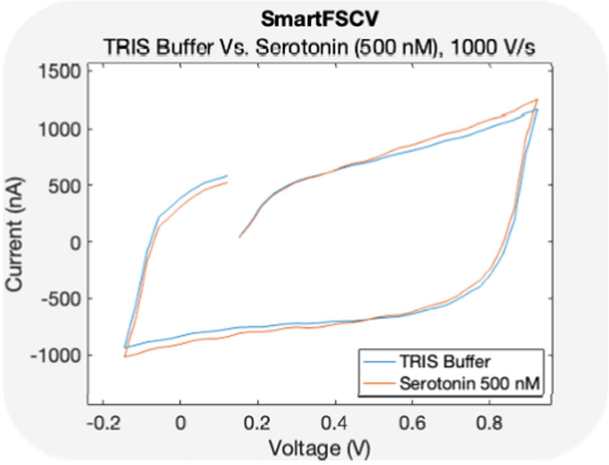


**Fig. 15.** SmartFSCV experiment 4 CV plot: TRIS Buffer Vs. serotonin (500 nM), 1000 V/s.

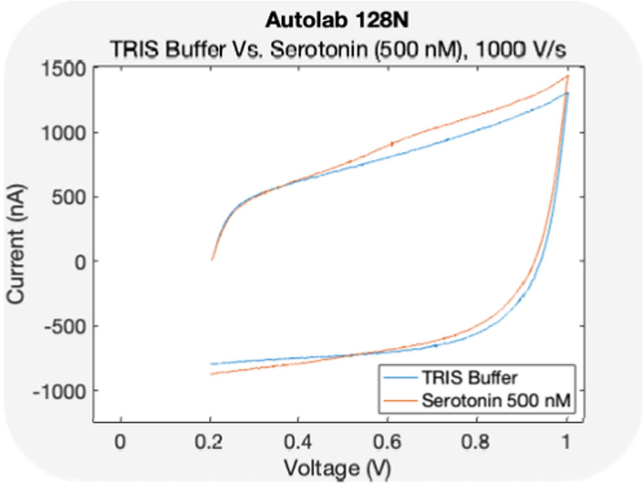


**Fig. 16.** Autolab 128N experiment 4 CV plot: TRIS Buffer Vs. serotonin (500 nM), 1000 V/s.

These results displayed a high accuracy of 100% and small loss of 0.02, potentially due to the low number of data samples tested. Thus, we conducted an additional AI experiment using more data. This algorithm has an inferencing time of 1 ms, peak RAM usage of 1.7 K and flash usage of 26.4 K.

### *D. Experiment 4: Secondary AI Detection of Serotonin*

The fourth experiment further evaluated the effectiveness of the AI detection of dynamic serotonin. A secondary AI algorithm was developed, again using unfiltered raw data, however, the output layers use 3 classes of no serotonin, 100 nM of serotonin and 500 nM of serotonin. Samples were collected using the same experimental procedure from Experiment 2, however, an additional sample using 500 nM of serotonin was collected. In addition, this experiment used 3 separate syringes loaded with a high volume of their diluted solution and removed the 6-port position valve. Each syringe was loaded into the syringe pump and allowed to flow into the flow cell for a minimum of 100 samples on the Autolab and SmartFSCV. This was done to collect more samples of the same solution for a longer duration, as the small sample loop provided limited time for data collection. A comparison between the results of SmartFSCV and the Autolab are displayed in Figs. 15 and 16.

These results displayed acceptable correlation between SmartFSCV and the Autolab. Measurement differences are potentially due to DAC inaccuracies of SmartFSCV ($\pm 2$ LSB maximum INL), the Autolab having a higher accuracy, and electrode drift due to SmartFSCV measuring after the Autolab. The Autolab did not measure below 0.2 V due to setup errors, therefore only the oxidation currents can be compared between devices. The main objective for this experiment was to compromise on optimal electrode conditions for a high data collection for training and testing the AI algorithm.

The dataset for the secondary algorithm contained 100 data samples of no serotonin (buffer), 100 nM serotonin, and 500 nM serotonin, totalling 300 samples. Data was split 79% for training and 21% for testing. The unfiltered raw data is time series based with a window of 1 ms per sample. Ideal training cycles and learning rates were previously found in the preliminary algorithm of 200 training cycles and a learning rate of 0.0001. This algorithm has an inferencing time of 4 ms, peak RAM usage of 1.9 K and flash usage of 26.7 K. Training results from the secondary AI algorithm are displayed in Table IV and Fig. 17 using 80 buffer samples, 80 serotonin samples of 500 nM, and 78 serotonin samples of 100 nM. Testing results from the secondary AI algorithm are displayed in Table V and Fig. 18 using 20 buffer

**TABLE IV**
TRAINING DATA CONFUSION MATRIX FOR SECONDARY AI

| | Buffer | 100 nM | 500 nM |
|---|---|---|---|
| Buffer | 92.9% | 7.1% | 0% |
| 100 nM | 12.5% | 68.8% | 18.8% |
| 500 nM | 0% | 11.1% | 88.9% |
| F1 Score | 0.90 | 0.73 | 0.86 |

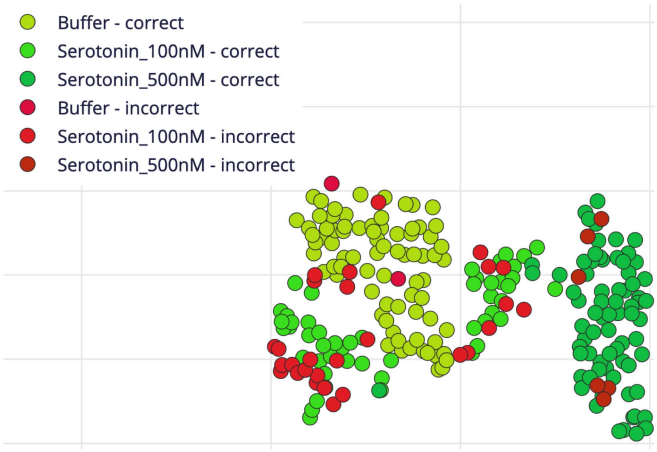


**Fig. 17.** Experiment 4: Secondary AI training results using 80 buffer samples, 80 serotonin samples of 500 nM, and 78 serotonin samples of 100 nM.

**TABLE V**
TESTING DATA CONFUSION MATRIX FOR SECONDARY AI

| | Buffer | 100 nM | 500 nM | Uncertain |
|---|---|---|---|---|
| Buffer | 80% | 15% | 0% | 5% |
| 100 nM | 4.5% | 81.8% | 4.5% | 9.1% |
| 500 nM | 0% | 0% | 100% | 0% |
| F1 Score | 0.86 | 0.84 | 0.98 | |

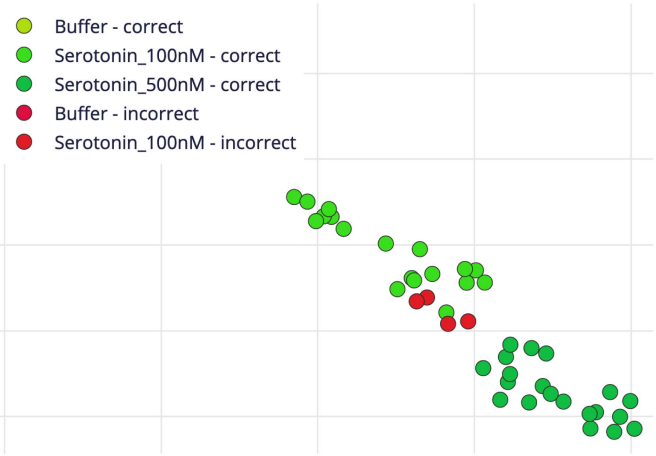


**Fig. 18.** Experiment 4: Secondary AI testing results using 20 buffer samples, 20 serotonin samples of 500 nM, and 22 serotonin samples of 100 nM.

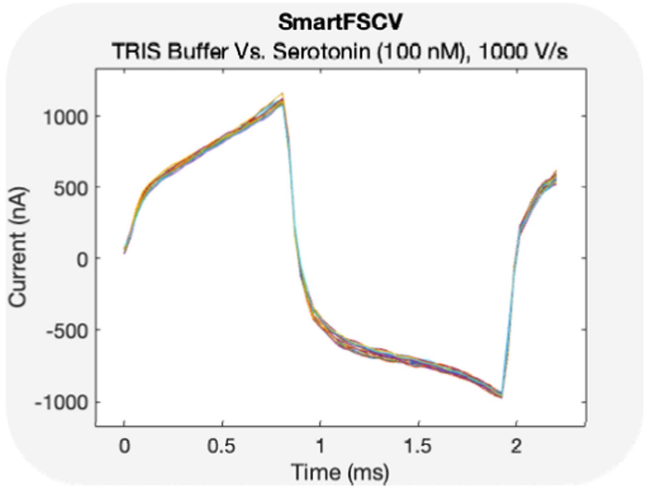


**Fig. 19.** Experiment 4: Time series plot: Raw TRIS buffer current (10 samples) Vs. serotonin (100 nM) current (10 samples), 1000 V/s.

samples, 20 serotonin samples of 500 nM, and 22 serotonin samples of 100 nM.

These results demonstrate sampling 100 points of data and then performing on-board AI is successful for determining if serotonin is present at different concentrations. Fig. 19 demonstrates some of the 300 raw data samples used in Experiment 4 of 10 buffer samples and 10 serotonin samples (100 nM). Without filtering, identification is difficult, however, the AI algorithm can identify to 83.3% accuracy with a loss of 0.43.

Because the AI can detect the serotonin using the raw data shown in Fig. 19, typical background subtracting CV plots are not necessary, thus opening the door to new single sweep measurement opportunities.

## IV. CONCLUSION

The underlying physiology of depression and the effects of SSRIs on the serotonergic system are currently not fully understood. Thus, research requires new tools to accurately measure serotonin levels in vivo and in vitro. This paper presented SmartFSCV, a miniaturised FSCV platform with on-board AI that targets serotonin. This device provides the first steps towards implementing AI algorithms on-board of a miniaturised FSCV device and offers the potential as a key analytical tool for neuroscientists. This work does not seek to replace the traditional benchtop FSCV systems, rather to introduce a potential wearable, battery operated device that can measure serotonin. SmartFSCV incorporates four key hardware components of: waveform generation, current measurement, processing system and power supply. Although successful, these four key hardware components have potential to be further refined, as limitations of the pandemic restricted access to ideal electronic components. In addition, AI capabilities on a miniaturised FSCV have not been done before. Thus, improvements such as more refined AI algorithms and further data collection for the training of better algorithms could be implemented. Furthermore, a software modification could give SmartFSCV the potential to sense for other neurochemicals such as dopamine and norepinephrine, as they require slower scan rates (400 V/s), lower than the maximum scan rate of the device (1000 V/s). In addition, the required voltage limits for dopamine and norepinephrine ($-0.4$ V to $+1.3$ V) are within the maximum voltage limits of the device ($-3$ V to $+3$ V). Nonetheless, SmartFSCV proved successful in using AI for serotonin identification and quantification from un-background subtracted signals, which has not been done before, and is a key first step to the continuous monitoring of serotonin, for the potential use in the treatment of neurological conditions.

## AUTHOR CONTRIBUTIONS

DMC, SDA, SJT, PH, MB and AZK, conception of the project. DMC, literature review. DMC and AZK, design of methodology and experimental protocol. DMC, circuit design. DMC, development. DMC, fabrication and evaluation. DMC, code development. DMC, experimental validation. EHD and BP, assistance with experimental validation. DMC, data collection. DMC, data analysis. DMC, drafting the manuscript. All authors contributed to the critical revision and finalisation of the manuscript.

## CONFLICT OF INTERESTS

The authors declare no potential conflicts of interest.

## REFERENCES

[1] P. Xu, Y. He, and Y. Xu, "Brain serotonin and energy homeostasis," *Serotonin*, pp. 307–334, 2019.

[2] M. Pourhamzeh et al., "The roles of serotonin in neuropsychiatric disorders," *Cellular Mol. Neurobiol.*, vol. 42, no. 6, pp. 1671–1692, Aug. 2022, doi: 10.1007/s10571-021-01064-9.
[3] E. J. Nestler, M. Barrot, R. J. DiLeone, A. J. Eisch, S. J. Gold, and L. M. Monteggia, "Neurobiology of depression," *Neuron*, vol. 34, pp. 13–25, 2002.
[4] C. A. Stockmeier et al., "Cellular changes in the postmortem hippocampus in major depression," *Biol. Psychiatry*, vol. 56, no. 9, pp. 640–650, Nov. 2004, doi: 10.1016/j.biopsych.2004.08.022.
[5] Y. I. Sheline, P. W. Wang, M. H. Gado, J. G. Csernansky, and M. W. Vannier, "Hippocampal atrophy in recurrent major depression," *Proc. Nat. Acad. Sci.*, vol. 93, no. 9, pp. 3908–3913, Apr. 1996.
[6] R. A. Saylor et al., "In vivo hippocampal serotonin dynamics in male and female mice: Determining effects of acute escitalopram using fast scan cyclic voltammetry," *Front. Neurosci.*, vol. 13, 2019, Art. no. 362, doi: 10.3389/fnins.2019.00362.
[7] A. Tundo et al., "Serotonin reuptake inhibitor-cognitive behavioural therapy-second generation antipsychotic combination for severe treatment-resistant obsessive-compulsive disorder. A prospective observational study," *Int. J. Psychiatry Clin. Pract.*, vol. 26, no. 4, pp. 395–400, Nov. 2022, doi: 10.1080/13651501.2022.2054351.
[8] H. Hatakama, N. Asaoka, K. Nagayasu, H. Shirakawa, and S. Kaneko, "A selective serotonin reuptake inhibitor ameliorates obsessive-compulsive disorder-like perseverative behavior by attenuating 5-HT(2C) receptor signaling in the orbitofrontal cortex," *Neuropharmacology*, vol. 206, Mar. 2022, Art. no. 108926, doi: 10.1016/j.neuropharm.2021.108926.
[9] D. Fluyau, P. Mitra, A. Jain, V. K. Kailasam, and C. G. Pierre, "Selective serotonin reuptake inhibitors in the treatment of depression, anxiety, and post-traumatic stress disorder in substance use disorders: A Bayesian meta-analysis," *Eur. J. Clin. Pharmacol.*, vol. 78, no. 6, pp. 931–942, Jun. 2022, doi: 10.1007/s00228-022-03303-4.
[10] A. K. Nohr et al., "Predictors and trajectories of treatment response to SSRIs in patients suffering from PTSD," *Psychiatry Res.*, vol. 301, Jul. 2021, Art. no. 113964, doi: 10.1016/j.psychres.2021.113964.
[11] F. Leichsenring, N. Heim, F. Leweke, C. Spitzer, C. Steinert, and O. F. Kernberg, "Borderline personality disorder: A review," *JAMA*, vol. 329, no. 8, pp. 670–679, Feb. 2023, doi: 10.1001/jama.2023.0589.
[12] A. C. Naglich, S. Bozeman, E. S. Brown, and B. Adinoff, "Effect of selective serotonin reuptake inhibitors on healthcare utilization in patients with post-traumatic stress disorder and alcohol use disorder," *Alcohol Alcoholism*, vol. 54, no. 4, pp. 428–434, Jul. 2019, doi: 10.1093/alcalc/agz045.
[13] J. Yuen et al., "Cocaine increases stimulation-evoked serotonin efflux in the nucleus accumbens," *J. Neurophysiol.*, vol. 127, no. 3, pp. 714–724, Mar. 2022, doi: 10.1152/jn.00420.2021.
[14] N. P. Gosmann et al., "Selective serotonin reuptake inhibitors, and serotonin and norepinephrine reuptake inhibitors for anxiety, obsessive-compulsive, and stress disorders: A 3-level network meta-analysis," *PLoS Med.*, vol. 18, no. 6, Jun. 2021, Art. no. e1003664, doi: 10.1371/journal.pmed.1003664.
[15] *Ketamine for Treatment-Resistant Depression : Neurobiology and Applications*. Amsterdam, The Netherlands: Elsevier, 2021.
[16] S. Jahanabadi, S. Amiri, M. Karkeh-Abadi, and A. Razmi, "Natural psychedelics in the treatment of depression; a review focusing on neurotransmitters," *Fitoterapia*, vol. 169, Sep. 2023, Art. no. 105620, doi: 10.1016/j.fitote.2023.105620.
[17] M. Hersey et al., "Inflammation-induced histamine impairs the capacity of escitalopram to increase hippocampal extracellular serotonin," *J. Neurosci.*, vol. 41, no. 30, pp. 6564–6577, Jul. 2021, doi: 10.1523/JNEUROSCI.2618-20.2021.
[18] G. Cattarinussi et al., "White matter microstructure associated with the antidepressant effects of deep brain stimulation in treatment-resistant depression: A review of diffusion tensor imaging studies," *Int. J. Mol. Sci.*, vol. 23, no. 23, Dec. 2022, Art. no. 15379, doi: 10.3390/ijms232315379.
[19] C. J. Thomson, R. A. Segrave, P. B. Fitzgerald, K. E. Richardson, E. Racine, and A. Carter, "Personal and relational changes following deep brain stimulation for treatment-resistant depression: A prospective qualitative study with patients and caregivers," *PLoS One*, vol. 18, no. 4, 2023, Art. no. e0284160, doi: 10.1371/journal.pone.0284160.
[20] G. N. Erjavec et al., "Serotonin 5-HT(2A) receptor polymorphisms are associated with irritability and aggression in conduct disorder," *Prog. Neuropsychopharmacol. Biol. Psychiatry*, vol. 117, Jul. 2022, Art. no. 110542, doi: 10.1016/j.pnpbp.2022.110542.
[21] A. Szeitz and S. M. Bandiera, "Analysis and measurement of serotonin," *Biomed. Chromatogr.*, vol. 32, no. 1, Jan. 2018, Art. no. e4135, doi: 10.1002/bmc.4135.
[22] P. J. Eugster et al., "Quantification of serotonin and eight of its metabolites in plasma of healthy volunteers by mass spectrometry," *Clinica Chimica Acta*, vol. 535, pp. 19–26, Aug. 2022, doi: 10.1016/j.cca.2022.08.012.
[23] J. Piestansky, M. Matuskova, I. Cizmarova, P. Majerova, A. Kovac, and P. Mikus, "Ultrasensitive determination of serotonin in human urine by a two dimensional capillary isotachophoresis-capillary zone electrophoresis hyphenated with tandem mass spectrometry," *J. Chromatogr. A*, vol. 1648, Jul. 2021, Art. no. 462190, doi: 10.1016/j.chroma.2021.462190.
[24] Y. Ikoma et al., "Measurement of changes in endogenous serotonin level by positron emission tomography with [18F]altanserin," *Ann. Nucl. Med.*, vol. 35, no. 8, pp. 955–965, Aug. 2021, doi: 10.1007/s12149-021-01633-4.
[25] C. Stucky and M. A. Johnson, "Improved serotonin measurement with fast-scan cyclic voltammetry: Mitigating fouling by SSRIs," *J. Electrochem. Soc.*, vol. 169, no. 4, Apr. 2022, doi: 10.1149/1945-7111/ac5ec3.
[26] M. I. Mauterer, P. M. Estave, K. M. Holleran, and S. R. Jones, "Measurement of dopamine using fast scan cyclic voltammetry in rodent brain slices," *Bio-Protocol*, vol. 8, no. 19, Oct. 2018, Art. no. e2473, doi: 10.21769/BioProtoc.2473.
[27] P. Puthongkham and B. J. Venton, "Recent advances in fast-scan cyclic voltammetry," *Analyst*, vol. 145, no. 4, pp. 1087–1102, Feb. 2020, doi: 10.1039/c9an01925a.
[28] J. G. Roberts and L. A. Sombers, "Fast-scan cyclic voltammetry: Chemical sensing in the brain and beyond," *Anal. Chem.*, vol. 90, no. 1, pp. 490–504, Jan. 2018, doi: 10.1021/acs.analchem.7b04732.
[29] P. Takmakov, C. J. McKinney, R. M. Carelli, and R. M. Wightman, "Instrumentation for fast-scan cyclic voltammetry combined with electrophysiology for behavioral experiments in freely moving animals," *Rev. Sci. Instrum.*, vol. 82, no. 7, Jul. 2011, Art. no. 074302, doi: 10.1063/1.3610651.
[30] D. M. Corva, S. D. Adams, K. E. Bennet, M. Berk, and A. Z. Kouzani, "Miniature FSCV devices: A review," *IEEE Sensors J.*, vol. 21, no. 12, pp. 13006–13018, Jun. 2021, doi: 10.1109/jsen.2021.3069950.
[31] Y. Ou, A. M. Buchanan, C. E. Witt, and P. Hashemi, "Frontiers in electrochemical sensors for neurotransmitter detection: Towards measuring neurotransmitters as chemical diagnostics for brain disorders," *Anal. Methods*, vol. 11, no. 21, pp. 2738–2755, Jun. 2019, doi: 10.1039/c9ay00055k.
[32] K. J. Christopher et al., "Wireless instantaneous neurotransmitter concentration sensing system (WINCS) for intraoperative neurochemical monitoring," presented at the 31st Annu. Int. Conf. of the IEEE EMBS, 2009.
[33] P. T. Inc., "8500-K2: Wireless rat FSCV system," 2019. [Online]. Available: https://store.pinnaclet.com/collections/wireless-fscv-systems
[34] S. D. Adams, E. H. Doeven, S. J. Tye, K. E. Bennet, M. Berk, and A. Z. Kouzani, "TinyFSCV: FSCV for the masses," *IEEE Trans. Neural Syst. Rehabil. Eng.*, vol. 28, no. 1, pp. 133–142, Jan. 2020, doi: 10.1109/TNSRE.2019.2956479.
[35] B. Bozorgzadeh, D. R. Schuweiler, M. J. Bobak, P. A. Garris, and P. Mohseni, "Neurochemostat: A neural interface SoC with integrated chemometrics for closed-loop regulation of brain dopamine," *IEEE Trans. Biomed. Circuits Syst.*, vol. 10, no. 3, pp. 654–667, Jun. 2016, doi: 10.1109/TBCAS.2015.2453791.
[36] B. P. Jackson, S. M. Dietz, and R. M. Wightman, "Fast-scan cyclic voltammetry of 5-hydroxytryptamine," *Anal. Chem.*, vol. 67, no. 6, pp. 1115–1120, 1995, doi: 10.1021/ac00102a015.
[37] "About keras." Accessed: Jun. 1, 2023. [Online]. Available: https://keras.io/about/
[38] "Advanced ML for every solution." Accessed: Jun. 1, 2023. [Online]. Available: https://www.edgeimpulse.com/
[39] M. Hexter, J. van Batenburg-Sherwood, and P. Hashemi, "Novel experimental and analysis strategies for fast voltammetry: 2. A troubleshoot-free flow cell for FSCV calibrations," *Amer. Chem. Soc. Meas. Sci. Au*, vol. 3, no. 2, pp. 120–126, Apr. 2023, doi: 10.1021/acsmeasuresciau.2c00059.